RESEARCH ARTICLE
SPACE PHYSICS: IONOSPHERIC PHYSICS

Earth and Planetary Physics
3: 481–488, 2019
doi: 10.26464/epp2019053

Anomaly distribution of ionospheric total electron content responses to some solar flares

HuiJun Le[1,2,3,4*], LiBo Liu[1,2,3,4], YiDing Chen[1,2,3,4], and Hui Zhang[1,2,3,4]

[1]Key Laboratory of Earth and Planetary Physics, Institute of Geology and Geophysics, Chinese Academy of Sciences, Beijing 100029, China;

[2]Innovation Academy of Earth Science, Chinese Academy of Sciences, Beijing 100029, China;

[3]Beijing National Observatory of Space Environment, Institute of Geology and Geophysics, Chinese Academy of Sciences, Beijing 100029, China;

[4]College of Earth and Planetary Sciences, University of the Chinese Academy of Sciences, Beijing 100049, China

Abstract: Previous studies have shown that the ionospheric responses to a solar flare are significantly dependent on the solar zenith angle (SZA): the ionospheric responses are negatively related to the SZAs. The largest enhancement in electron density always occurs around the subsolar point. However, from 2001 to 2014, the global distribution of total electron content (TEC) responses showed no obvious relationship between the increases in TEC and the SZA during some solar flares. During these solar flares, the greatest enhancements in TEC did not appear around the subsolar point, but rather far away from the subsolar point. The distribution of TEC enhancements showed larger TEC enhancements along the same latitude. The distribution of anomalous ionospheric responses to the solar flares was not structured the same as traveling ionospheric disturbances. This anomaly distribution was also unrelated to the distribution of background neutral density. It could not be explained by changes in the photochemical process induced by the solar flares. Thus, the transport process could be one of the main reasons for the anomaly distribution of ionospheric responses to the solar flares. This anomaly distribution also suggests that not only the photochemical process but also the transport process could significantly affect the variation in ionospheric electron density during some solar flares.

Keywords: solar flare; ionospheric response; transport process

Citation: Le, H. J., Liu, L. B., Chen, Y. D., Zhang, H. (2019). Anomaly distribution of ionospheric total electron content responses to some solar flares. *Earth Planet. Phys.*, *3*(6), 481–488. http://doi.org/10.26464/epp2019053

1. Introduction

Solar flares can cause a sudden enhancement in solar irradiation ranging from X-rays to extreme ultraviolet (EUV) rays. During flares, the sudden enhanced solar irradiation produces extra ionization in the ionosphere. These extra ionizations cause electron density enhancements from low to high heights. Thus, the total electron content (TEC) also shows significant enhancements, which manifest as sudden increases in TEC (SITEC). The rapid development of global positioning systems (GPSs) and the corresponding GPS receiving stations have opened a new era in which ionospheric TEC can be measured. Using GPS TEC data, scientists have carried out many studies on the ionospheric responses to solar flares (e.g., Afraimovich, 2000; Le HJ et al., 2007, 2011, 2013; Leonovich et al., 2002, 2010; Liu JY et al., 2004, 2006; Mendillo and Evans, 1974; Tsurutani et al., 2005; Wan WX et al., 2005; Xiong B et al., 2011, 2014, 2016, 2019; Zhang DH and Xiao Z, 2005; Zhang DH et al., 2002, 2011). Wan WX et al. (2005) analyzed GPS data during the July 14, 2000, flare and studied the SITEC. They found that both the rate of variation and the enhancement in TEC were proportional to the flare radiation and inversely proportional to the Chapman function. Tsurutani et al. (2005) reported a significant enhancement of more than 15 TEC units (TECU, 10^{16} electron/m^2) for several hours during the X17.2 solar flare on October 28, 2003.

The solar zenith angle (SZA) is an important factor in the ion production rate. A smaller SZA results in a larger ionization rate. In general, the photochemical process is considered the most important factor in the short time change of solar EUV rays. Thus, the global distribution of ionospheric responses to a solar flare is significantly dependent on the SZA. The largest enhancement in electron density is around the subsolar region and the smallest is around the sunset region. Zhang DH et al. (2002) reported that, as a whole, the sudden enhancement in TEC caused by the solar flare on July 14, 2000, increased as the SZA decreased. Le HJ et al. (2013) further investigated the dependence of the SZA on the SITEC by analyzing global TEC enhancements for more than 100 solar flare events. Some modeling studies have also shown that the SZA has an important effect on the ionospheric responses to solar flares (Pawlowski and Ridley, 2008, 2011; Qian LY et al., 2010; Le HJ et al., 2007, 2016). In this study, we found that TEC enhancements were not significantly dependent on the SZA for some solar flare events, including the X1.6 flare on October 19, 2001, the X1.2 flare on October 22, 2001, the X1.1 flare on October 19, 2003, the X2.0 flare on November 7, 2004, the X6.2 flare on September

Correspondence to: H. J. Le, lehj@mail.iggcas.ac.cn
Received 21 SEP 2019; Accepted 09 OCT 2019.
Accepted article online 24 OCT 2019.

9, 2005, the X2.1 flare on September 10, 2005, and the X3.1 flare on October 24, 2014, which means other factors were affecting the ionospheric responses to the solar flare. The global distribution of TEC enhancements during these solar flares were analyzed, and the possible factors that may have influenced the effects of the solar flare on the ionosphere are discussed.

2. Data Sources

Global positioning system-derived TEC data were used to study the global distribution of ionospheric responses to solar flares. Solar radiation for the nightside ionosphere does not change; thus, we calculated the variation in the TEC derived from the sunlit-side GPS receivers to monitor the ionospheric TEC variations during the solar flares. The raw TEC values were integrated TEC values from a certain GPS satellite to a receiver station on the ground, which usually was a slant TEC. The slant TEC was converted to a vertical TEC by assuming an ionospheric spherical shell at an altitude of 350 km. To reduce the error of the transformation from the slant TEC to the vertical TEC, we used only the TEC data derived from the satellite with a median elevation angle during solar flares greater than 40°. To obtain the variation in the TEC induced by a solar flare for each observed TEC series, we calculated the background TEC values by fitting the curve of the TEC before and after a solar flare. We then calculated the enhancement of the TEC by subtracting this background value from the TEC series. The peak enhancement (ΔTEC) was used to describe the TEC responses to the solar flare.

3. Results and Discussion

As previous studies have pointed out (Afraimovich, 2000; Wan WX et al., 2005; Le HJ et al., 2007, 2013, 2015; Manju et al., 2012), the SZA is an important factor in the ionospheric responses to solar flares. Thus, one can expect to find the greatest enhancement in electron density around the subsolar point during a solar flare. We analyzed the global distribution of SITEC for more than 100 X-class solar flares in 2001–2006. Although most of the solar flares were significantly dependent on the SZA, the ionospheric responses for several flares did not show such an SZA dependence, including the X1.6 flare on October 19, 2001, the X1.2 flare on October 22, 2001, the X1.1 flare on October 19, 2003, the X2.0 flare on Novem-

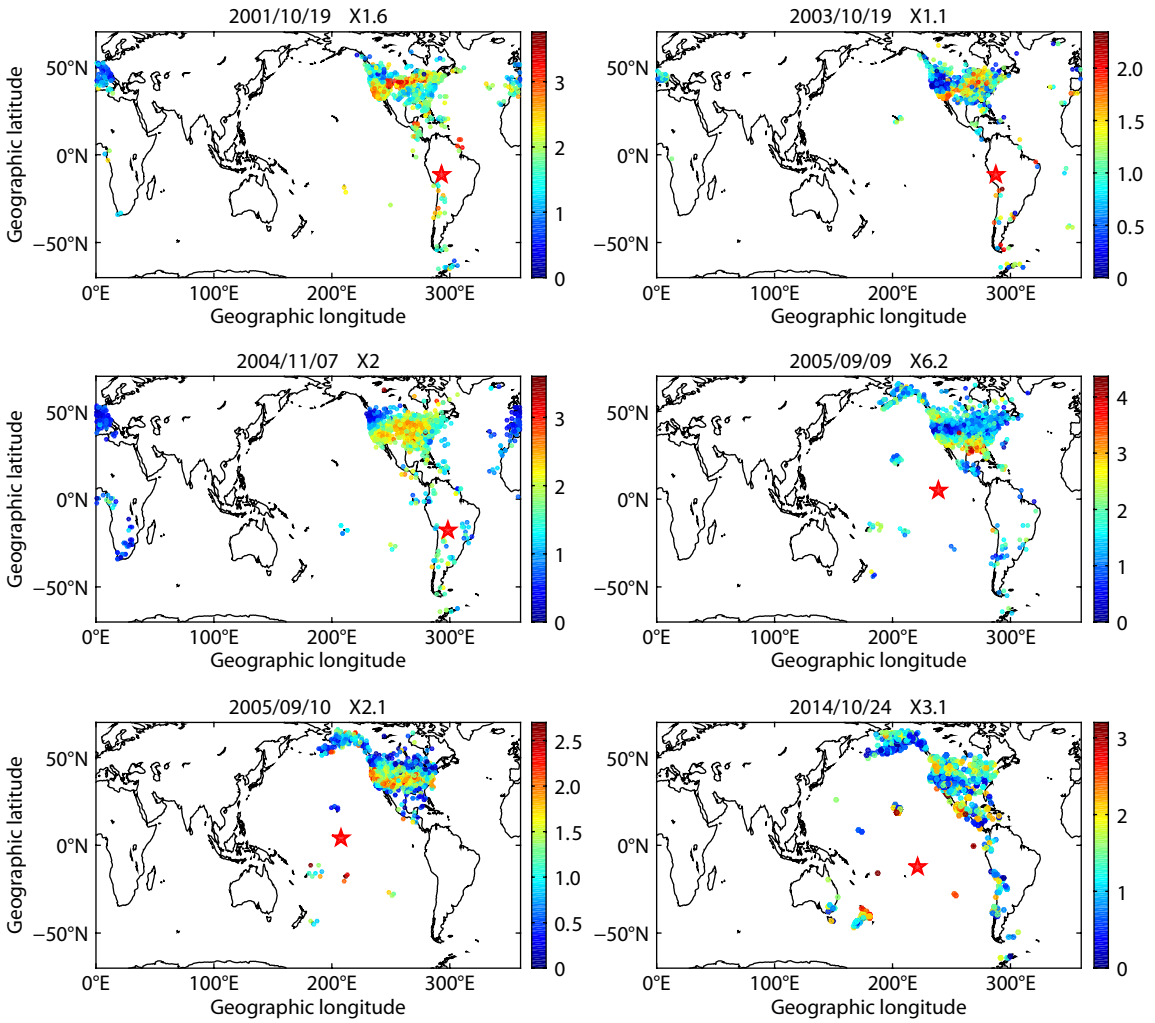

Figure 1. Global distribution of ΔTEC in the dayside for the six solar flares on October 19, 2001, October 19, 2003, November 7, 2004, September 9, 2005, September 10, 2005, and October 24, 2014. The solid pentagram denotes the subsolar point. The color represents the magnitude of the ΔTEC, in TEC units (10^{16} electron/m^2).

ber 7, 2004, the X6.2 flare on September 9, 2005, the X2.1 flare on September 10, 2005, and the X3.1 flare on October 24, 2014.

Figure 1 illustrates the spatial distribution of ΔTEC during six solar flare events. The ionospheric electron density responses to a solar flare mainly appeared in the dayside because no changes occurred in the solar EUV flux for the nighttime. The ΔTEC values in the nighttime were almost zero; thus, only the ΔTEC values in the daytime are shown. Because of limitations in the figure, the results for the X1.2 flare on October 22, 2001, are not shown here. One can observe that during the six solar flares, the greatest enhancements in TEC did not occur at a subsolar point, but rather far away from the subsolar point. The region of large ΔTEC seemed to be a zonal belt located in the same latitude. Furthermore, during the solar flares on October 19, 2003, and September 9, 2005, the spatial distribution of the ΔTEC showed a wave-like structure. Figure 2 illustrates plots of the ΔTEC versus the cosine of the SZA (cos(χ)) for the six solar flares. As reported by Le HJ et al. (2013), a high linear correlation exists between the ΔTEC and cos(χ) for most solar flares. However, Figure 2 shows that the correlation coefficients between them for the six solar flares were very low, which means the SZA was not the main controlling factor in the distribution of ΔTEC values during the six solar flares. Other factors significantly affected the ionospheric responses to the solar flares, although the linear fitting lines still showed that, on the whole, the larger SZAs caused smaller ionospheric responses.

To further check the anomaly distribution of ionospheric responses to the solar flares, we calculated the temporal variations in ΔTEC in the different regions. For example, Figure 3 illustrates the temporal variations in ΔTEC in the four regions with different SZA during the solar flare on September 9, 2009. In the region of longitudes 250°–270° and latitudes 15°–20°, the mean SZA was 24.25°. We could not find an apparent TEC enhancement in this region, nor could we find a remarkable ΔTEC. In the region of longitudes 250°–270° and latitudes 25°–30°, the mean SZA was 33.68°. In this region, we did find a significant TEC enhancement as well as a remarkable ΔTEC. The mean ΔTEC value for all the observations in this region was approximately 3 TECU. In the region farther from the subsolar point (longitudes 240°–250° and latitudes 36°–42°, with a mean SZA of 40.06°), the TEC enhancement again became smaller, with a mean ΔTEC value of approximately

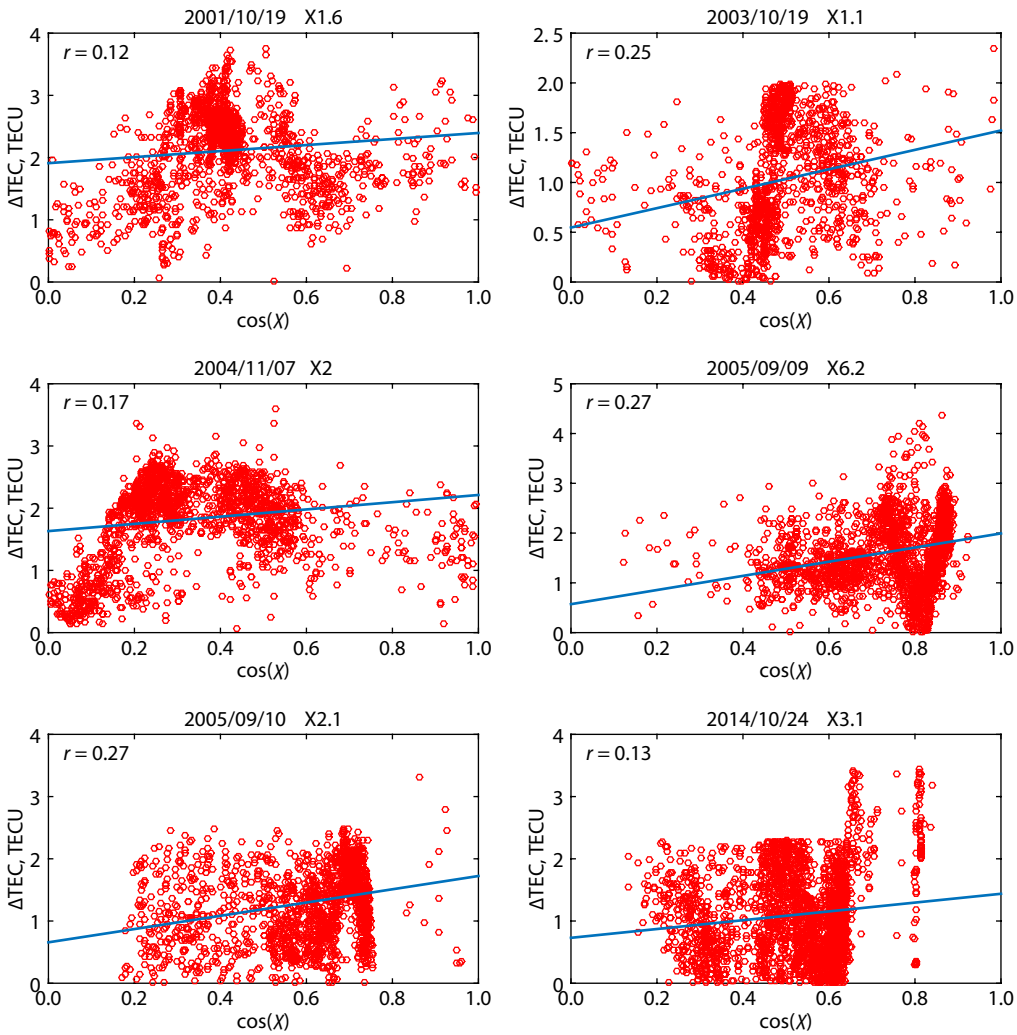

Figure 2. Scatter plots of the observed ΔTEC versus cosine of the solar zenith angle (cos(χ)) for the six solar flares on October 19, 2001, October 19, 2003, November 7, 2004, September 9, 2005, September 10, 2005, and October 24, 2014. The solid lines represent the linear fitting. The corresponding correlation coefficient between the ΔTEC and cos(χ) is shown in each panel.

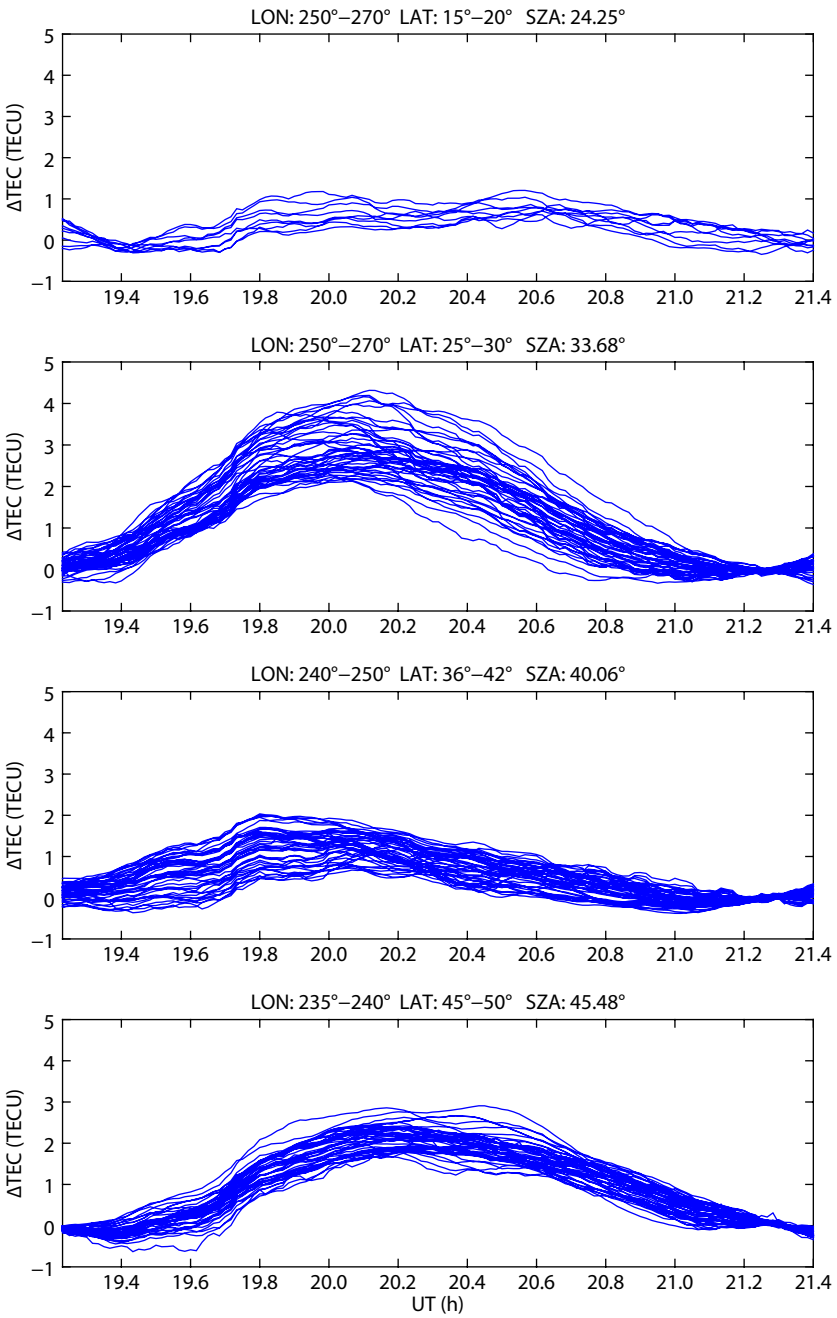

Figure 3. Temporal variations in the ΔTEC in four regions with different solar zenith angles (SZA) during the solar flare on September 9, 2005. Detailed information on the longitude and latitude and the SZA is shown in each panel. UT, universal time; TECU, TEC units (10^{16} electron/m^2).

1 TECU. Finally, in the region of longitudes 230°–240° and latitudes 45°–50°, the mean SZA was 45.48°. We found that the TEC enhancement again became larger when the mean ΔTEC value was approximately 1.8 TECU.

The results illustrated in Figure 3 show the smallest ΔTEC in the region with the smallest SZA value, and the fluctuation of the ΔTEC shows a wave-like structure. To further show the temporal and spatial variation of ionospheric responses to the solar flare on September 9, 2005, we plotted the global distribution of ΔTEC at various universal times (UT), as shown in Figure 4. The figure shows that the high and low ΔTEC values always appeared in the same places, which means the fluctuation of the ΔTEC was not due to wave propagation, as occurs in traveling ionospheric disturbances. Thus, the zonal distribution of ΔTEC may have been due to the combined effect of an EUV enhancement and other effects. In addition to calculating the global distribution of ΔTEC values for the solar flare on September 9, 2005, we calculated the global distribution of ΔTEC values at various UT for the other five solar flares. The locations of the high and low ΔTEC values during these solar flares did not change. The evolution of ΔTEC during the other five flares was similar to that on September 9, 2005.

As reported in previous studies, the ionospheric responses to sudden enhancements of solar EUV rays during a solar flare should be related to the SZA. According to the Chapman ionization theory, a

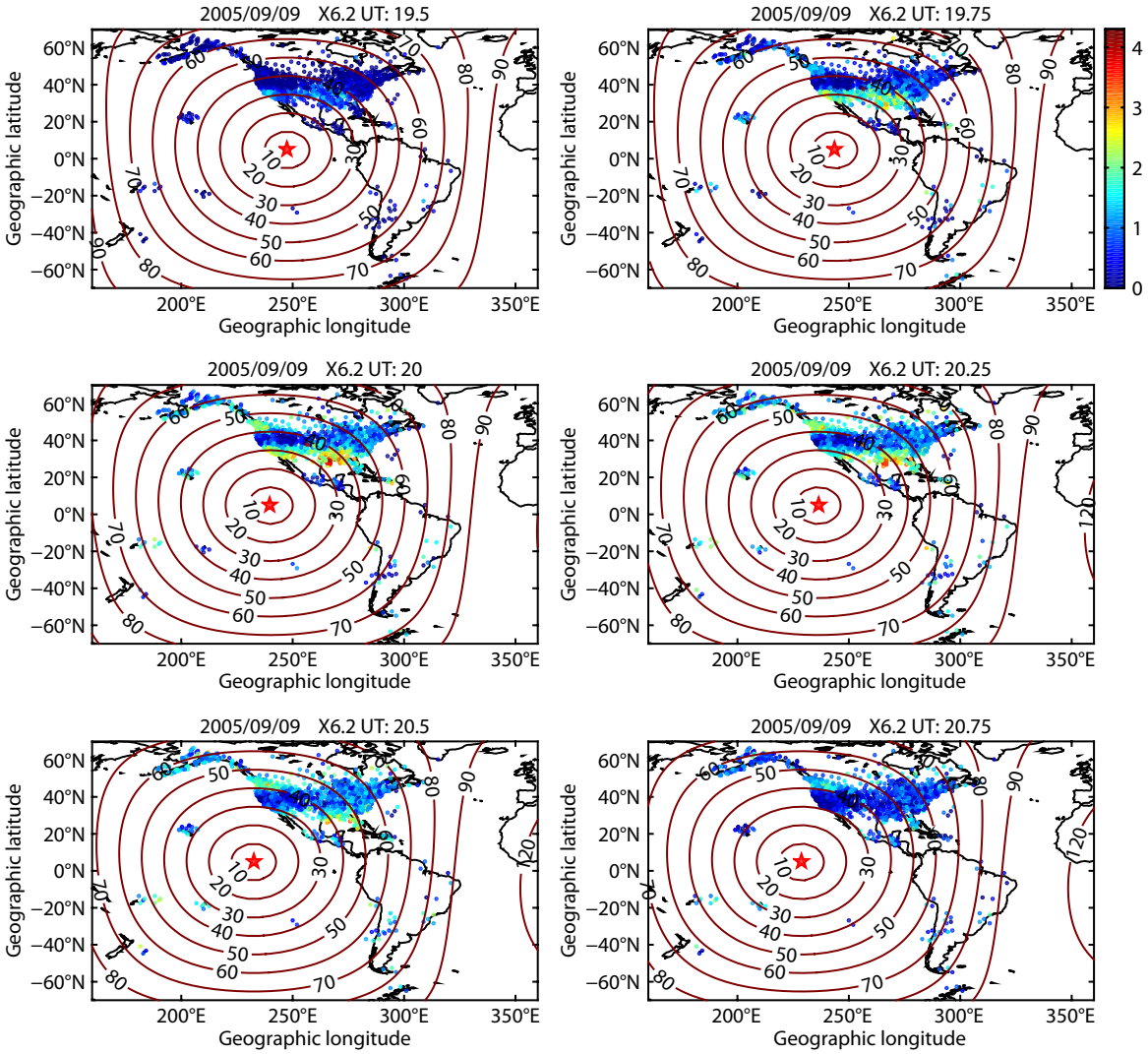

Figure 4. Global distribution of ΔTEC at various universal times (UT) from 19.5 UT to 20.75 UT for the solar flare on September 9, 2005. Contour lines of the solar zenith angle are plotted in each panel.

smaller SZA would result in a greater production of electrons. The duration of a sudden increase in solar EUV rays during a solar flare is in the range of several minutes to several tens of minutes. Because the photochemical process is much faster than the transport process during a solar flare, the effect of the transport process is usually neglected. Thus, we can find a significant dependence of the ΔTEC on the SZA during most solar flares. However, we found no apparent relationship between the ΔTEC values and the SZA during the six solar flares, as illustrated in Figure 2. In addition, according to the balance of the photochemical process, the electron density is positively related to the ratio O/N_2. Figure 5 illustrates the distribution of the column number density ratio O/N_2 during the hours around the flare time for the flares on October 19, 2003, November 7, 2004, September 9, 2005, and September 10, 2005. These data are derived from the Global Ultraviolet Imager (GUVI) aboard the Thermosphere–Ionosphere–Mesosphere Energetics and Dynamics (TIMED) satellite, which was launched on December 7, 2001. For the distribution of O/N_2 on November 7, 2004, we can see a larger value in North America than in South America. Such a distribution of O/N_2 is similar to that of the ΔTEC. But during the solar flare, the SZA in North America was much larger than that in South America. The mean SZA in the region of North America with high ΔTEC values reached about 70°. As shown in Figure 5, the greater value of O/N_2 in North America was not enough to cause the much larger ΔTEC in the region than at the subsolar point. Figure 5 also shows that no significant anomaly distributions in O/N_2 occurred during the other three solar flares. Thus, the anomaly distribution of ionospheric responses to the solar flares was unrelated to the distribution of the background neutral density.

As mentioned, the photochemical process could not have produced the anomaly distribution of ionospheric responses during the six solar flares. In addition, some studies have suggested that the electrodynamic process at low latitudes could have been influenced by the sudden enhancements in solar irradiances (e.g., Qian LY et al., 2012; Nogueira et al., 2015; Zhang RL et al., 2017), which could have caused a weaker eastward electric field and a weakened equatorial ionization anomaly (EIA) crest structure. The two EIA crests would be located at the lower latitudes. Such a weakened EIA would cause a change in the latitudinal structure in

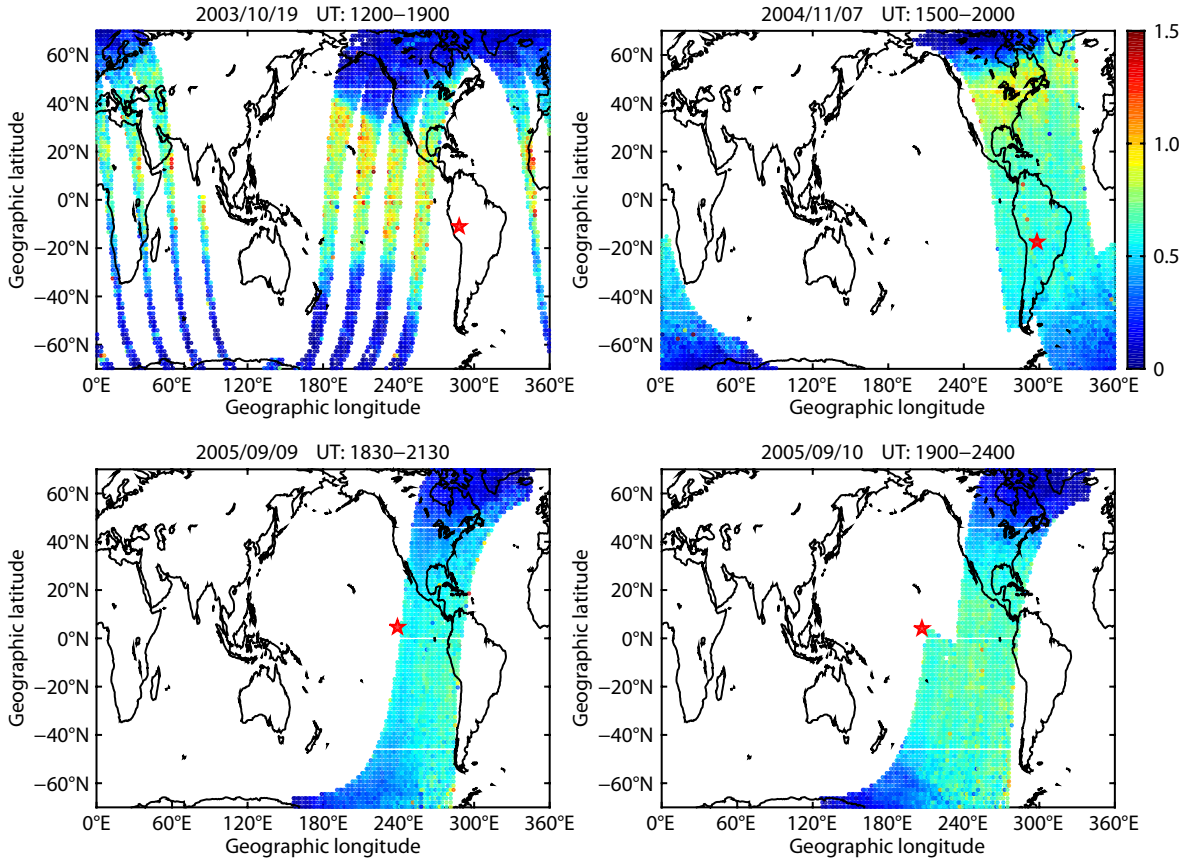

Figure 5. Column number density ratio O/N_2 derived from the Global Ultraviolet Imager (GUVI) observations during the time near the flare times for the flares on October 19, 2003, November 7, 2004, September 9, 2005, and September 10, 2005. UT, universal time.

the middle- and low-latitude regions. The region equatorward of the EIA crest would have fewer enhancements in the TEC and the region poleward of the EIA crest would have more enhancements in the TEC. In addition, some studies (Le HJ et al., 2015; Pawlowski and Ridley, 2011) have shown that solar flares would result in changes in the horizontal neutral wind. The strength of a neutral wind would be different and the effects of a neutral wind on the vertical drift of plasma would also be different at different latitudes because of the differences in geomagnetic inclination. Thus, a change in the neutral wind would also cause different electron density variations along the different latitudes. Additionally, the plasma transport process resulting from a change in the eastward electric field and the horizontal neutral wind might play an important role in the anomaly distribution. However, we lacked the observations of plasma transport process like the ion drift velocity in the F_2 region during these solar flares to support the explanation for the anomaly distribution. Thus, the main process in the anomaly distribution is still unclear. In addition, it is interesting to note that all the anomaly distributions in the ΔTEC during the six solar flares occurred mainly in the region of North America and that these solar flares occurred in the three months of September, October, and November.

It should be noted that significant geomagnetic disturbances occurred during the six solar flares. Figure 6 shows the variations in the *Kp* index and the *Dst* index on the days of the six solar flares. Many studies (e.g., Foster, 1993; Maruyama, 2006; Yizengaw et al., 2006; Coster and Skone, 2009; Zou SS et al., 2013, 2014; Cherniak et al., 2015) have reported that the storm-time enhanced density (SED) occurs at middle and high latitudes during medium- and large-sized magnetic storms. The SED is characterized by a plume of enhanced ionospheric electron density. However, the TEC enhancement patterns during the six solar flares took the form of narrow zonal belts along the same latitudes. Furthermore, we found no SED events during these solar flares. Thus, as discussed, the TEC enhancements during the solar flares (Figure 1) were not affected by SED events. However, as shown in Figure 6, significant geomagnetic disturbances during the six solar flares could possibly have affected the plasma transport process because of electrical field and neutral wind changes. During geomagnetic storms, the ionosphere, especially in the North American sector, tends to be affected because this region is closer to the north magnetic pole than are other longitudinal sectors. Thus, the anomaly distribution in ΔTEC values may be due to the combined effect of EUV enhancements and a disturbed transport process.

4. Summary

In this study, the global distribution of solar flare effects on the ionosphere were investigated by using GPS TEC data. We found anomaly distributions in ΔTEC values for seven solar flares: the X1.6 flare on October 19, 2001, the X1.2 flare on October 22, 2001, the X1.1 flare on October 19, 2003, the X2.0 flare on November 7, 2004, the X6.2 flare on September 9, 2005, the X2.1 flare on

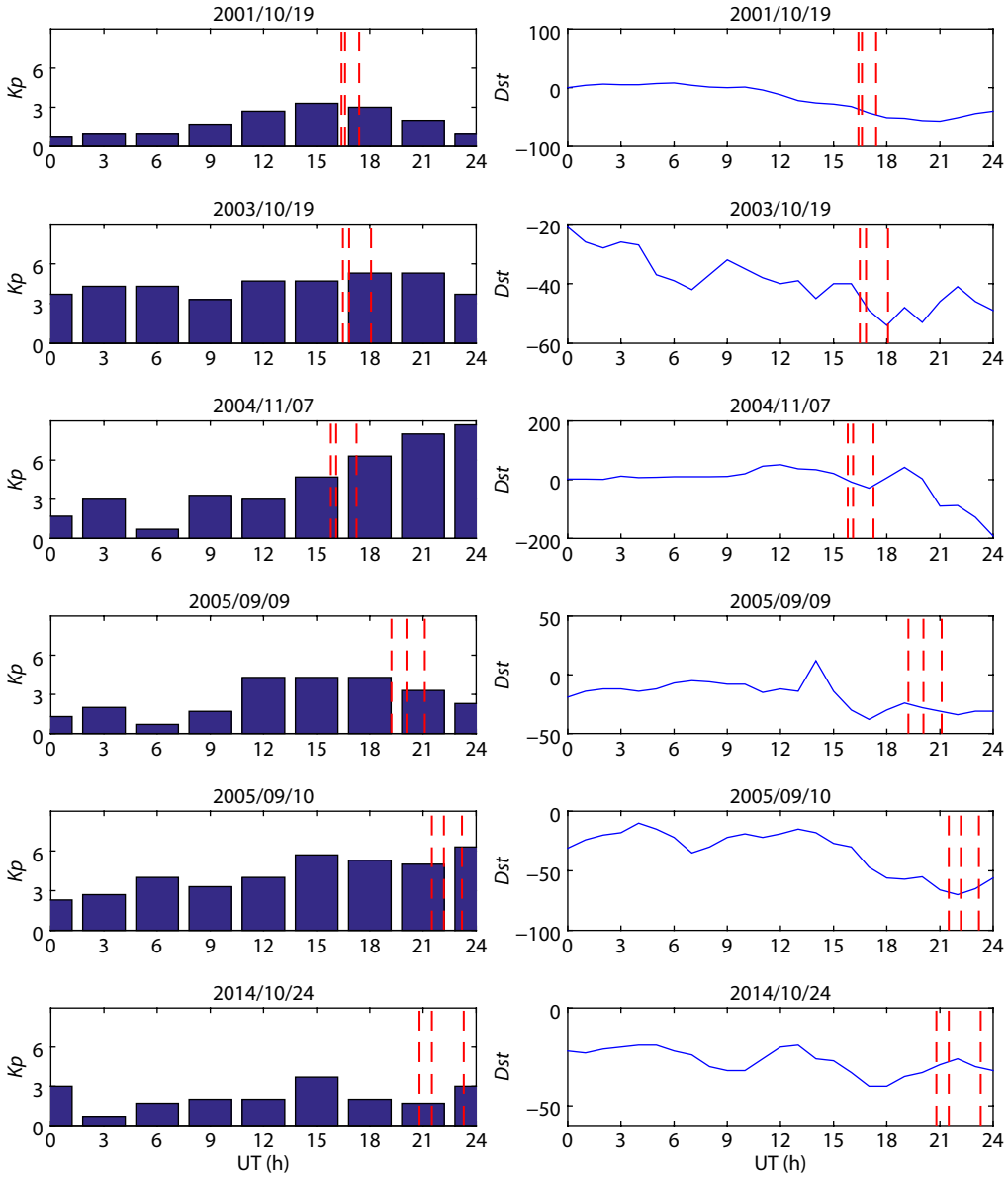

Figure 6. Variations in the *Kp* index and *Dst* index on the days of the six solar flares. The three dashed lines indicate the start, peak, and end times of the solar flares. UT, universal time.

September 10, 2005, and the X3.1 flare on October 24, 2014. The enhancements in TEC were not significantly dependent on the SZA during these solar flares. The largest was not around the subsolar point, but rather far away from the subsolar point. The region with the largest TEC enhancements seemed to be a zonal belt along the same latitude. Spatial analysis of the TEC enhancements showed that such an anomaly distribution was not due to traveling ionospheric disturbances, and the anomaly distribution was not related to the background neutral density. The transport process may be the cause of the anomaly distribution, but no observed data could be used to explain this phenomenon. In addition, it should be noted that the anomaly distributions of TEC enhancements during the six solar flares occurred mainly in the region of North America and that the flares appeared in September, October, and November. Significant geomagnetic disturbances during the six solar flares possibly affected the plasma transport process. The anomaly distribution of TEC enhancements may therefore be due to the combined effect of an enhancement in EUV rays and a disturbed transport process.

Acknowledgments

This research was supported by the National Key Research and Development Program (2018YFC1503504), the National Natural Science Foundation of China (41822403, 41621063, 41774165), and the Youth Innovation Promotion Association CAS. The raw GPS TEC data were obtained from the Goddard Space Flight Center (ftp://cddis.gsfc.nasa.gov/glonass/data/daily/). The data on the column number density ratio O/N_2 were obtained from TIMED/GUVI (http://guvi.jhuapl.edu/).

References

Afraimovich, E. L. (2000). GPS global detection of the ionospheric response to solar flares. *Radio Sci.*, *35*(6), 1417–1424.

https://doi.org/10.1029/2000RS002340

Cherniak, I., Zakharenkova, I., and Redmon, R. J. (2015). Dynamics of the high-latitude ionospheric irregularities during the 17 March 2015 St. Patrick's Day storm: Ground-based GPS measurements. *Space Weather*, *13*(9), 585–597. https://doi.org/10.1002/2015SW001237

Coster, A., and Skone, S. (2009). Monitoring storm-enhanced density using IGS reference station data. *J. Geod.*, *83*(3-4), 345–351. https://doi.org/10.1007/s00190-008-0272-3

Foster, J. C. (1993). Storm time plasma transport at middle and high latitudes. *J. Geophys. Res.*, *98*(A2), 1675–1689. https://doi.org/10.1029/92JA02032

Le, H. J., Liu, L. B., Chen, B., Lei, J. H., Yue, X. N., and Wan, W. X. (2007). Modeling the responses of the middle latitude ionosphere to solar flares. *J. Atmos. Sol. Terr. Phys.*, *69*(13), 1587–1598. https://doi.org/10.1016/j.jastp.2007.06.005

Le, H. J., Liu, L. B., He, H., and Wan, W. X. (2011). Statistical analysis of solar EUV and X-ray flux enhancements induced by solar flares and its implication to upper atmosphere. *J. Geophys. Res.*, *116*(A11), A11301. https://doi.org/10.1029/2011JA016704

Le, H. J., Liu, L. B., Chen, Y. D., and Wan, W. X. (2013). Statistical analysis of ionospheric responses to solar flares in the solar cycle 23. *J. Geophys. Res.*, *118*(1), 576–582. https://doi.org/10.1029/2012JA017934

Le, H. J., Ren, Z. P., Liu, L. B., Chen, Y. D., and Zhang, H. (2015). Global thermospheric disturbances induced by a solar flare: a modeling study. *Earth Planets Space*, *67*, 3. https://doi.org/10.1186/s40623-014-0166-y

Le, H. J., Liu, L. B., Ren, Z. P., Chen, Y. D., Zhang, H., and Wan, W. X. (2016). A modeling study of global ionospheric and thermospheric responses to extreme solar flare. *J. Geophys. Res.*, *121*(1), 832–840. https://doi.org/10.1002/2015JA021930

Leonovich, L. A., Afraimovich, E. L., Romanova, E. B., and Taschilin, A. V. (2002). Estimating the contribution from different ionospheric regions to the TEC response to the solar flares using data from the international GPS network. *Ann. Geophys.*, *20*(12), 1935–1941. https://doi.org/10.5194/angeo-20-1935-2002

Leonovich, L. A., Tashchilin, A. V., and Portnyagina, O. Y. (2010). Dependence of the ionospheric response on the solar flare parameters based on the theoretical modeling and GPS data. *Geomagn. Aeronomy*, *50*(2), 201–210. https://doi.org/10.1134/S0016793210020076

Liu, J. Y., Lin, C. H., Tsai, H. F., and Liou, Y. A. (2004). Ionospheric solar flare effects monitored by the ground-based GPS receivers: theory and observation. *J. Geophys. Res.*, *109*(A1), A01307. https://doi.org/10.1029/2003JA009931

Liu, J. Y., Lin, C. H., Chen, Y. I., Lin, Y. C., Fang, T. W., Chen, C. H., Chen, Y. C., and Hwang, J. J. (2006). Solar flare signatures of the ionospheric GPS total electron content. *J. Geophys. Res.*, *111*(A5), A05308. https://doi.org/10.1029/2005JA011306

Manju, G., Simi, K. G., and Nayar, S. R. P. (2012). Analysis of solar EUV and X-ray flux enhancements during intense solar flare events and the concomitant response of equatorial and low latitude upper atmosphere. *J. Atmos. Sol. Terr. Phys.*, *86*, 1–5. https://doi.org/10.1016/j.jastp.2012.05.008

Maruyama, T. (2006). Extreme enhancement in total electron content after sunset on 8 November 2004 and its connection with storm enhanced density. *Geophys. Res. Lett.*, *33*(20), L20111. https://doi.org/10.1029/2006GL027367

Mendillo, M., and Evans, J. V. (1974). Incoherent scatter observations of the ionospheric response to a large solar flare. *Radio Sci.*, *9*(2), 197–203. https://doi.org/10.1029/RS009i002p00197

Nogueira, P. A. B., Souza, J. R., Abdu, M. A., Paes, R. R., Sousasantos, J., Marques, M. S., Bailey, G. J., Denardini, C. M., Batista, I. S., … Chen, S. S. (2015). Modeling the equatorial and low-latitude ionospheric response to an intense X-class solar flare. *J. Geophys. Res.*, *120*(4), 3021–3032. https://doi.org/10.1002/2014JA020823

Pawlowski, D. J., and Ridley, A. J. (2008). Modeling the thermospheric response to solar flares. *J. Geophys. Res.*, *113*(A10), A10309. https://doi.org/10.1029/2008JA013182

Pawlowski, D. J., and Ridley, A. J. (2011). The effects of different solar flare characteristics on the global thermosphere. *J. Atmos. Sol. Terr. Phys.*, *73*(13), 1840–1848. https://doi.org/10.1016/j.jastp.2011.04.004

Qian, L. Y., Burns, A. G., Chamberlin, P. C., and Solomon, S. C. (2010). Flare location on the solar disk: modeling the thermosphere and ionosphere response. *J. Geophys. Res.*, *115*(A9), A09311. https://doi.org/10.1029/2009JA015225

Qian, L. Y., Burns, A. G., Solomon, S. C., and Chamberlin, P. C. (2012). Solar flare impacts on ionospheric electrodyamics. *Geophys. Res. Lett.*, *39*(6), L06101. https://doi.org/10.1029/2012GL051102

Tsurutani, B. T., Judge, D. L., Guarnieri, F. L., Gangopadhyay, P., Jones, A. R., Nuttall, J., Zambon, G. A., Didkovsky, L., Mannucci, A. J., … Viereck, R. (2005). The October 28, 2003 extreme EUV solar flare and resultant extreme ionospheric effects: comparison to other Halloween events and the Bastille Day event. *Geophys. Res. Lett.*, *32*(3), L03S09. https://doi.org/10.1029/2004GL021475

Wan, W. X., Liu, L. B., Yuan, H., Ning, B. Q., and Zhang, S. R. (2005). The GPS measured SITEC caused by the very intense solar flare on July 14, 2000. *Adv. Space Res.*, *36*(12), 2465–2469. https://doi.org/10.1016/j.asr.2004.01.027

Xiong, B., Wan, W. X., Liu, L. B., Withers, P., Zhao, B. Q., Ning, B. Q., Wei, Y., Le, H. J., Ren, Z. P., … Liu, J. (2011). Ionospheric response to the X-class solar flare on 7 September 2005. *J. Geophys. Res.*, *116*(A11), A11317. https://doi.org/10.1029/2011JA016961

Xiong, B., Wan, W. X., Ning, B. Q., Ding, F., Hu, L. H., and Yu, Y. (2014). A statistic study of ionospheric solar flare activity indicator. *Space Wea.*, *12*(1), 29–40. https://doi.org/10.1002/2013SW001000

Xiong, B., Wan, W. X., Yu, Y., and Hu, L. H. (2016). Investigation of ionospheric TEC over China based on GNSS data. *Adv. Space Res.*, *58*(6), 867–877. https://doi.org/10.1016/j.asr.2016.05.033

Xiong, B., Li, X. L., Wan, W. X., She, C. L., Hu, L. H., Ding, F., and Zhao, B. Q. (2019). A method for estimating GNSS instrumental biases and its application based on a receiver of multisystem. *Chinese J. Geophys.* (*in Chinese*), *62*(4), 1199–1209. https://doi.org/10.6038/cjg2019M0318

Yizengaw, E., Moldwin, M. B., and Galvan, D. A. (2006). Ionospheric signatures of a plasmaspheric plume over Europe. *Geophys. Res. Lett.*, *33*(17), L17103. https://doi.org/10.1029/2006GL026597

Zhang, D. H., Xiao, Z., and Chang, Q. (2002). The correlation of flare's location on solar disc and the sudden increase of total electron content. *Chin. Sci. Bull.*, *47*(1), 83–85. https://doi.org/10.1360/02tb9017

Zhang, D. H., and Xiao, Z. (2005). Study of ionospheric response to the 4B flare on 28 October 2003 using international GPS service network data. *J. Geophys. Res.*, *110*(A3), A03307. https://doi.org/10.1029/2004JA010738

Zhang, D. H., Mo, X. H., Cai, L., Zhang, W., Feng, M., Hao, Y. Q., and Xiao, Z. (2011). Impact factor for the ionospheric total electron content response to solar flare irradiation. *J. Geophys. Res.*, *116*(A4), A04311. https://doi.org/10.1029/2010JA016089

Zhang, R. L., Liu, L. B., Le, H. J., and Chen, Y. D., (2017). Equatorial ionospheric electrodynamics during solar flares. *Geophys. Res. Lett.*, *44*(10), 4558–4565. https://doi.org/10.1002/2017GL073238

Zou, S. S., Ridley, A. J., Moldwin, M. B., Nicolls, M. J., Coster, A. J., Thomas, E. G., and Ruohoniemi, J. M. (2013). Multi-instrument observations of SED during 24-25 October 2011 storm: Implications for SED formation processes. *J. Geophys. Res.*, *118*(12), 7798–7809. https://doi.org/10.1002/2013JA018860

Zou, S. S., Moldwin, M. B., Ridley, A. J., Nicolls, M. J., Coster, A. J., Thomas, E. G., and Ruohoniemi, J. M. (2014). On the generation/decay of the storm-enhanced density plumes: role of the convection flow and field-aligned ion flow. *J. Geophys. Res.*, *119*(10), 8543–8559. https://doi.org/10.1002/2014JA020408